



HAL
open science

A novel methodology to estimate the importance of isotopic exchange in the CH₃I adsorption by impregnated activated carbons

Mouheb Chebbi, Hantao Lin, B. Azambre, Celine Monsanglant Louvet, Benoit Marcillaud, Audrey Roynette, Denis Doizi

► To cite this version:

Mouheb Chebbi, Hantao Lin, B. Azambre, Celine Monsanglant Louvet, Benoit Marcillaud, et al.. A novel methodology to estimate the importance of isotopic exchange in the CH₃I adsorption by impregnated activated carbons. *Separation and Purification Technology*, 2024, 330 (Part C), pp.125427. 10.1016/j.seppur.2023.125427 . irsn-04594761

HAL Id: irsn-04594761

<https://irsn.hal.science/irsn-04594761>

Submitted on 30 May 2024

HAL is a multi-disciplinary open access archive for the deposit and dissemination of scientific research documents, whether they are published or not. The documents may come from teaching and research institutions in France or abroad, or from public or private research centers.

L'archive ouverte pluridisciplinaire **HAL**, est destinée au dépôt et à la diffusion de documents scientifiques de niveau recherche, publiés ou non, émanant des établissements d'enseignement et de recherche français ou étrangers, des laboratoires publics ou privés.



Distributed under a Creative Commons Attribution - NonCommercial - NoDerivatives 4.0 International License



A novel methodology to estimate the importance of isotopic exchange in the CH₃I adsorption by impregnated activated carbons

M. Chebbi^{a,*}, H. Lin^a, B. Azambre^{b,*}, C. Monsanglant-Louvet^a, B. Marcillaud^a, A. Roynette^a, D. Doizi^c

^a Institut de Radioprotection et de Sécurité Nucléaire (IRSN), PSN-RES, Saclay, 91192 Gif-sur-Yvette, France

^b Université de Lorraine, Laboratoire de Chimie et Physique-Approche Multi-Echelle des Milieux Complexes (LCP-A2MC, EA n°4362), Institut Jean-Barriol FR2843 CNRS, ICPM, 1, Bd Arago, F-57500 Saint-Avold, France

^c Commissariat à l'Énergie Atomique (CEA), DEN/DES/ISAS/DRMP/SPC/LRMO, Gif-sur-Yvette, 91191, France

ARTICLE INFO

Handling Editor: Z Bao

Keywords:

Carbonaceous materials
Radioactive methyl iodide
Iodine capture
Breakthrough curve
Decontamination factors
Potassium iodide

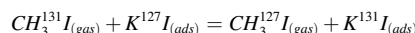
ABSTRACT

Activated Carbons (AC) are widely used in the ventilation lines of nuclear facilities for the removal of volatile iodine species. In this paper, new experimental methodologies have been developed in order to measure the BreakThrough Curves (BTC) of both radioactive and stable CH₃I for KI- or TEDA- impregnated AC {T = 20 – 30 °C, dry conditions}. Non-impregnated and KI-impregnated AC were shown to display similar performances for the trapping of stable CH₃¹²⁷I. In that case, only physical interactions within the micropores were involved in the adsorption process. A significant improvement of the retention occurred after TEDA impregnation. Regarding the trapping of the γ -labelled CH₃I, a significant enhancement of AC performances during both retention and breakthrough phases is observed after KI impregnation due to the promotion of isotopic exchange phenomenon. Therefore, the contribution of KI, still rarely studied in the literature, was isolated for the first time from the other mechanisms (physisorption and chemisorption). The in-depth analysis of BTC data obtained under active and inactive conditions allowed quantifying the contribution due to isotopic exchange.

1. Introduction

The development of nuclear industry in France and worldwide has arisen debates due to the possible occurrence of severe nuclear accidents. More particularly, Chernobyl (1986) and Fukushima (2011) disasters have resulted in dramatic consequences in terms of radioactive releases to the environment and population contamination. Hence, the efficient capture of radioactive species potentially released from nuclear facilities in all scenarios, *i.e.* from normal operating conditions to degraded situations, remains a major concern to improve nuclear safety and the acceptability of nuclear energy. Among the fission products potentially emitted, a special attention should be paid to iodine because of its high radiological impact towards the thyroid gland as well as its high volatility (mainly as I₂ and/or organic iodides, CH₃I being the main representative) [1,2]. In that respect, Activated Carbon (AC) is largely used within the nuclear ventilation networks [3] of nuclear facilities to capture these volatile iodine species. Owing to its well-developed microporosity [4] ($d_{\text{pore}} < 2$ nm), the *nuclear grade* AC used in iodine traps is known to display a high removal efficiency under normal

conditions, as well as simple design and low maintenance costs. However, the AC performances for CH₃I trapping are drastically reduced under humid conditions due to the competitive adsorption between water vapor and CH₃I [5]. In that respect, the performances of AC for CH₃I retention can be further improved by impregnation with organic or inorganic compounds. The most employed impregnants in the nuclear field [6] are triethylenediamine (TEDA, ≤ 5 wt%) and potassium iodide (KI, 1 wt%), which interact with CH₃I through different mechanisms [7–11]. On the one hand, it has been claimed that TEDA reacts with CH₃I through chemisorption processes involving the formation of molecular complexes or quaternary ammonium species according to the relative humidity [10,11]. On the other hand, the presence of potassium iodide was reported to induce an isotopic exchange reaction with radioactive CH₃I, this process being summarized by the following equation [12]:



Despite the historical use of KI as impregnant in nuclear adsorbents, its relative contribution for the capture of CH₃I under different

* Corresponding authors.

E-mail addresses: mouheb.chebbi@irsn.fr (M. Chebbi), bruno.azambre@univ-lorraine.fr (B. Azambre).

<https://doi.org/10.1016/j.seppur.2023.125427>

Received 2 August 2023; Received in revised form 6 October 2023; Accepted 17 October 2023

Available online 28 October 2023

1383-5866/© 2023 Elsevier B.V. All rights reserved.

experimental conditions is not well documented, especially from a quantitative viewpoint.

In French nuclear facilities, an annual test of iodine traps equipping the ventilation networks is performed to check their efficiency towards volatile iodine species. These annual tests are performed in presence of $\text{CH}_3^{131}\text{I}$ and paradoxically induces the major release of radioactive iodine to the environment. Therefore, the replacement of this traditional testing procedure by a novel non-radioactive method is an important challenge in the field of radioprotection. However, the validity and the on-site implementation of such a non-radioactive method relies on two important points:

- (i) the implementation of a sufficiently sensitive analytical method for $\text{CH}_3^{127}\text{I}$ detection as compared with the method by γ -spectrometry used in the case of $\text{CH}_3^{131}\text{I}$. In that respect, it is worth recalling that the accuracy of decontamination factors DF ($\text{DF} = C_{\text{in}}/C_{\text{out}}$) measured to assess the filter performance both depends on the upstream CH_3I concentration as well as the limits of the detection method, which could be reached in the measurement of the downstream CH_3I concentration.
- (ii) the second one implies to specifically quantify the contribution of isotopic exchange in the overall trapping process, which involves also physisorption and chemisorption phenomena.

During our previous work [13], the isotopic exchange reaction with KI was more clearly observed only under humid conditions and ambient temperature ($T = 20\text{ }^\circ\text{C}$, $\text{HR} = 90\%$), *i.e.* in conditions where physisorption and chemisorption were altered. In this study, our efforts were directed towards providing an initial quantification of the contribution due to isotopic exchange.

In the first part, the main properties of the investigated adsorbents, as deduced from several characterizations, are given. In the second part, the analysis of the breakthrough curves obtained for both stable and radioactive CH_3I will be discussed. Finally, a novel methodology to quantify the contribution of isotopic exchange to the overall trapping process will be presented and discussed.

2. Experimental

2.1. Materials and physico-chemical characterizations

Several commercial AC materials obtained from coconut shells and impregnated with different contents in KI or TEDA were used in this study.

These AC samples were fully characterized during our previous investigation [13]. UV-Visible spectrophotometry, X-ray photoelectron spectroscopy (XPS) analysis, X-ray diffraction (XRD) analysis, scanning electron microscopy with energy dispersive X-ray spectroscopy (SEM/EDX) analysis, N_2 and H_2O adsorption-desorption isotherms were employed in order to gain insights about their chemical, textural, and structural features. In this paper, only a brief summary of these characterization data is presented in Section 3.1. For details about the employed procedures and other results obtained, the reader can refer to [13].

2.2. CH_3I gas-phase dynamic adsorption test benches

The adsorption behavior of the investigated AC towards both stable and γ -labelled CH_3I adsorption were investigated through two different sets of BTC measurements: one for the stable $\text{CH}_3^{127}\text{I}$, while the other (newly designed) is dedicated to the γ -labelled $\text{CH}_3^{127+131}\text{I}$. Operating conditions used in these two set-ups were kept mostly similar in order to warranty the comparison between these two configurations.

The main characteristics of each tested experimental configuration are summarized in Figure S1 (ESI)

2.2.1. Measurement of breakthrough curves (BTC) with stable CH_3I

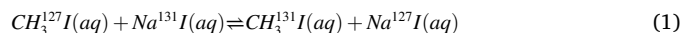
The BTC measurements using stable $\text{CH}_3^{127}\text{I}$ were carried out using the BRIOCH test bench [14] whose principle is given in Figure S2, ESI.

Briefly, the AC sample is prepared using a cylindrical sample holder with an inner diameter of 25 mm and a bed height of 50 mm, thanks to the procedure described in our previous study [13]. Prior to each experiment, the AC sample (mass about 10 g) was grinded to 1–1.4 mm in order to avoid preferential schemes [15]. An *ex-situ* pretreatment of the AC at $100\text{ }^\circ\text{C}$ overnight was also performed to remove most of the humidity within the tested adsorbents. The AC sample holder was fed by an inlet CH_3I concentration of 10 ppmv/air, generated from certified CH_3I gas bottles (Air Products, $[\text{CH}_3\text{I}] = 160\text{ ppmv} \pm 0.5\%/\text{N}_2$) and pressurized air. The CH_3I concentration and total flow rate ($6.63\text{ L}\cdot\text{min}^{-1}$ (NTP), corresponding to a linear velocity of $25\text{ cm}\cdot\text{s}^{-1}$ at $30\text{ }^\circ\text{C}$), are in agreement with conditions met in nuclear effluents [16] and allowed to obtain a complete BTC in less than 50 h. The outlet line of the AC sample holder was connected to a gas chromatograph (Clarus 680, PerkinElmer) equipped with a high-sensitivity PDECD (Valco instruments) specific for halogenated compounds detection. The GC-PDECD system is equipped with two slightly polar columns (Rtx-502.2, RESTEK) composed of 5% diphenyl and 95% dimethyl polymethyl siloxane. Analytical parameters were optimized to obtain high-quality BTC. These parameters as well as calibration curves are presented in supplementary section (see S3 in ESI).

2.2.2. Measurements with γ -labelled CH_3I

A newly designed experimental set-up for γ -labelled CH_3I breakthrough curve (BTC) measurement was developed in the present study (Fig. 1).

Part A of the experimental set-up is dedicated to the generation of γ -labelled CH_3I steady flow using a permeation method. This method involves the isotopic exchange of iodine molecules in liquid phase between the $\text{CH}_3^{127}\text{I}$ (1 mL) and $\text{Na}^{131}\text{I}/\text{Na}^{127}\text{I}$ solution (10 MBq) according to the following reaction [17]:



The generated γ -labelled CH_3I in liquid phase is then transferred into the permeation tube for the gas generation. More precisely, the permeation tube is placed in the oven ($T = 80\text{ }^\circ\text{C}$) under flowing conditions (dilution flow 1 = $0.4\text{ L}/\text{min}$ NTP, Fig. 1). After at least 8 h of equilibration, a stable amount of γ -labelled CH_3I is diffused into the vapor phase thanks to the permeable membrane of the tube wall. The dilution flow 2 (Air) is used to regulate the total flowrate to $6.86\text{ L}\cdot\text{min}^{-1}$ (NTP) to obtain a linear velocity of $25\text{ cm}\cdot\text{s}^{-1}$ at $T = 20\text{ }^\circ\text{C}$ at the inlet of the tested adsorbents (part C, Fig. 1). With the aim to achieve a total concentration of 10 ppmv at the outlet of the part A, the dilution flow 1 is fed by stable CH_3I ($[\text{CH}_3\text{I}] = 160\text{ ppmv}/\text{N}_2$). In this configuration, the resulted ratio between the ^{131}I and ($^{131}\text{I} + ^{127}\text{I}$) in the γ -labelled CH_3I flux (defined as the isotopic dilution factor (G_{IDF})), is about 8×10^{-11} .

In Fig. 1, part B is a “bypass section” designed to monitor the flow of γ -labelled CH_3I at the inlet of the bed adsorbent. Part C is the “adsorption test section” and allows for continuous samplings at the outlet of the tested AC, so that BTC could be generated up to sorbent saturation by CH_3I . For the sampling, the flow of γ -labelled CH_3I passes through commercial cartridges for a certain duration, and those cartridges are changed regularly to be measured by γ -spectrometry. Details about γ -spectrometry measurement and calibration are presented in the supplementary section (see S4). Overall, the $\text{CH}_3^{131}\text{I}$ flowrate ($\text{Bq}\cdot\text{min}^{-1}$) can be determined either in the “bypass” or “adsorption” sections. However, it was needed to include two pathways in parts B and C to warranty a continuous generation of γ -labelled CH_3I during the manual change of a given cartridge.

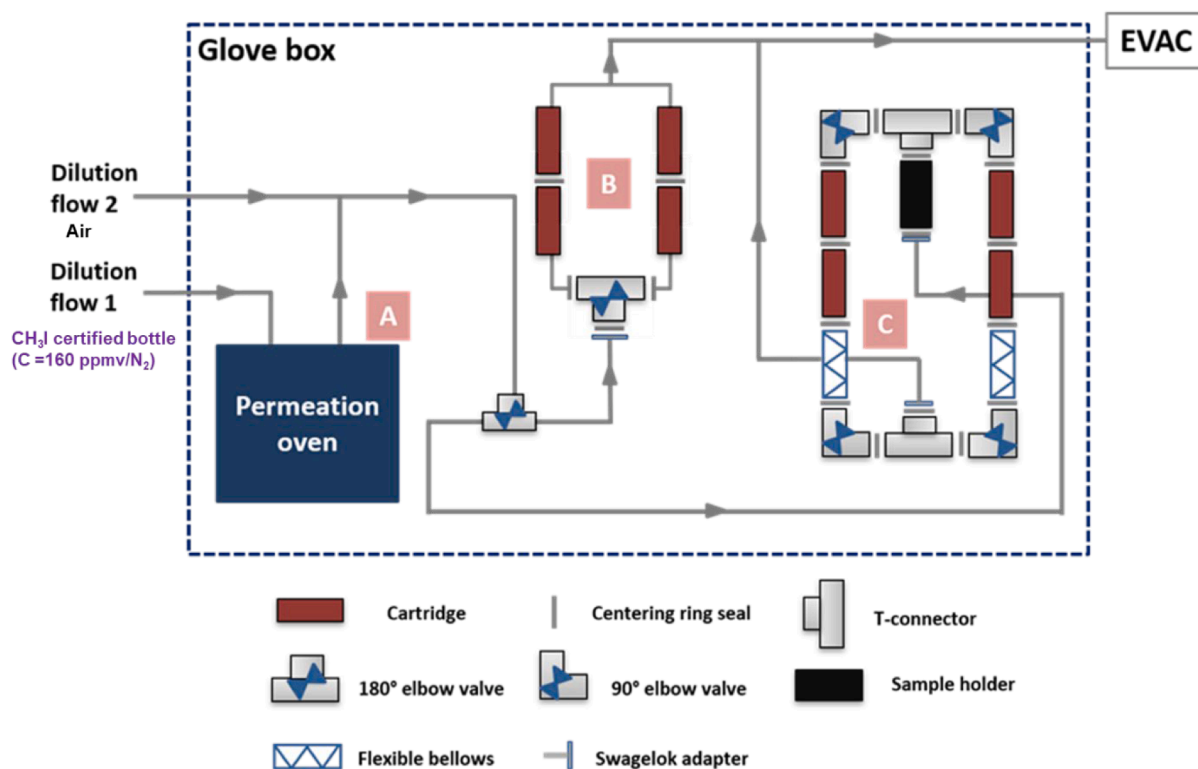


Fig. 1. Schematic view of the experimental set-up for γ -labelled CH_3I BTC measurement.

2.3. Data processing

The quantification of the isotopic exchange contribution requires further processing of BTC data thanks to an appropriate dynamic adsorption model. The objective is to calculate the transient adsorption capacities at different levels of saturation for both radioactive and non-radioactive methyl iodide. In that respect, an improved equation proposed in the literature, based on the original Thomas model [18], was used in the present study because it considers the non-symmetric nature of BTC. Hence, this so-called “log-Thomas model”, was expressed from the following equation [19]:

$$\ln\left(\frac{C_{inlet}}{C_{outlet}} - 1\right) = K_{Th} \ln\left(\frac{Q_{Th} m}{D}\right) - K_{Th} \ln(C_{inlet} t) \quad (1)$$

Where C_{inlet} concentration at the adsorbent bed inlet (mol/m^3);
 C_{outlet} concentration at the adsorbent bed outlet (mol/m^3);
 K_{Th} Thomas rate constant, considered as a purely empirical parameter ($\text{m}^3 \cdot \text{mol}^{-1} \cdot \text{h}^{-1}$);
 Q_{Th} adsorption capacity at saturation ($\text{mol} \cdot \text{g}^{-1}$);
 m adsorbent mass (g);
 D volume flowrate ($\text{L} \cdot \text{h}^{-1}$).

In addition, the use of this improved equation may be a good alternative to overcome the lack of experimental points at low saturation levels for radioactive methyl iodide (see an example in ESI for 5% KI AC, S5).

The adsorption capacity at a 5% breakthrough ($Q_{5\%}$) [10,16] is also determined in order to estimate the useful working capacity displayed by the sorbent. The $Q_{5\%}$ is calculated from the fitted curve of improved Thomas model according to the following equation:

$$Q_{5\%} = \frac{M(\text{CH}_3\text{I}) \times D \times \int_0^{t_{5\%}} (C_{inlet} - C_{outlet}) dt}{m} \quad (2)$$

Where $Q_{5\%}$ adsorption capacity at 5% breakthrough ($\text{mg} \cdot \text{g}^{-1}$);

$M(\text{CH}_3\text{I})$ molar mass of CH_3I ($\text{mg} \cdot \text{mol}^{-1}$);

$t_{5\%}$ time (min) at $C_{outlet} = 5\% \times C_{inlet}$, calculated from the log-Thomas model equation;

m Adsorbent mass (g).

The existence of diffusional constraints within the tested adsorbents was evaluated through the length of mass transfer zone (MTZ) calculated from the following equation [20]:

$$\frac{L_T}{L} = \frac{t_{95\%} - t_{5\%}}{t_{95\%}} \quad (3)$$

Where L bed length (cm);

L_T length of mass transfer zone (cm);

$t_{95\%}$ time at $C_{outlet} = 95\% \times C_{inlet}$ as deduced from the improved Thomas equation (s);

$t_{5\%}$ time at $C_{outlet} = 5\% \times C_{inlet}$ as deduced from the improved Thomas equation (s).

When L_T is small compared with L , most of the adsorption capacity has been successfully used until the breakthrough. Therefore, a narrow value of L_T/L is required for an effective use of the adsorbent [20].

3. Results and discussion

3.1. Porosimetric properties of the investigated adsorbents

The porosimetric properties of the tested materials are reported in the supplementary (S8). According to our previous study [13], the impregnated TEDA and KI entities were found to be well dispersed within the internal porosity of activated carbons without significant aggregation on the external surface. As deduced from N_2 porosimetry at 77 K (S6), high specific surface areas (around 1000–1200 m^2/g) were measured for all AC samples, with an important contribution of the micropores to the overall porosity (>94%).

All KI-impregnated carbons (0.1–5 wt%) display rather similar specific surface area and microporosity which indicates that impregnation of KI has no influence at contents inferior to 5 wt% (or 0.4 % in molar ratio with reference to carbon, S6). However, a slightly negative impact of triethylenediamine (TEDA) impregnant can be noticed on the S_{BET} and V_{micro} values, especially at contents equal to 3 wt% or higher (S6). The decrease in textural properties may be related to the presence of TEDA entities within the micropores or at their openings [10,21].

3.2. Performances of AC adsorbents towards the trapping of stable CH_3I

The obtained BTC for the tested AC are presented in Fig. 2. The adsorption capacities ($Q_{5\%}$ and Q_{th}), mass transfer zone lengths (MTZ) and model parameters (K_{th}) as computed from the log-Thomas model, are summarized in Table 1.

Under the employed conditions ($C_{\text{inlet}} = 10$ ppmv, $T = 30$ °C, bed height = 50 mm, linear velocity = $25 \text{ cm}\cdot\text{s}^{-1}$, residence time = 0.2 s), $\text{CH}_3^{127}\text{I}$ is totally retained by the non-impregnated AC (NI) for 5 h (Fig. 2, red squares), corresponding to a decontamination factor (DF) of about 12,600 (C_{inlet}/DL). Subsequently, the penetration P ($100 \times C_{\text{outlet}}/C_{\text{inlet}}$) increases progressively until reaching the complete saturation of the adsorbent bed ($P = 100$ %) after around 12 h (Fig. 2). This results in adsorption capacities at 5 % breakthrough ($Q_{5\%}$) and saturation (Q_{th}) of 14.1 of $22.1 \text{ mg}\cdot\text{g}^{-1}$ respectively (Table 1). These adsorption capacities are in line with the reported performances for non-impregnated AC with similar porosimetric properties under rather similar operating conditions [22]. Nevertheless, these measured values using an inlet CH_3I concentration of 10 ppmv are much lower than the maximal CH_3I adsorption capacity of the same AC ($\sim 200 \text{ mg/g}$) derived from adsorption isotherm measured from batch reactor studies with CH_3I concentrations up to 1000 ppmv, $T = 35$ °C, $\text{HR} \approx 30$ % [23].

For all the AC with KI contents between 0 and 5 wt%, rather similar retention performances can be deduced from their quasi-overlapping BTC (Fig. 2). This is in agreement with their similar textural properties (see S6). Nevertheless, a decrease in adsorption capacity can be noticed in the case of 5 %KI/AC (7 % and 17 % of decrease in Q_{th} and $Q_{5\%}$ respectively). The slightly hindered affinity of this sorbent for CH_3I has to be related either to a decrease of the amount of adsorption sites or to an increase in hydrophilicity of the AC with KI content, as reported in our previous study [13]. Indeed, the presence of residual humidity in the vicinity of KI entities may represent a physical barrier for methyl iodide

Table 1

Summary of computed adsorption parameters (from the modeling of btc data) for stable CH_3I ($C_{\text{inlet}} = 10$ ppmv, $T = 30$ °C, bed height = 50 mm, linear velocity = $25 \text{ cm}\cdot\text{s}^{-1}$, residence time = 0.2 s, reference mass = 10 g).

AC type	$Q_{5\%}$ ($\text{mg}\cdot\text{g}^{-1}$)	Q_{th} ($\text{mg}\cdot\text{g}^{-1}$)	K_{th} ($\text{m}^3\cdot\text{mol}^{-1}\cdot\text{h}^{-1}$)	R^2	MTZ
NI	14.0	21.3	7.42	0.9989	55 %
0.1 %KI/AC	14.4	21.6	7.59	0.9995	54 %
0.5 %KI/AC	14.8	23.4	6.75	0.9986	58 %
1 %KI/AC	14.1	22.4	6.68	0.9991	59 %
2 %KI/AC	13.5	21.7	6.46	0.9992	60 %
5 %KI/AC	11.6	19.9	5.65	0.9987	65 %
3 %TEDA/AC	33.7	47.2	9.28	0.9968	47 %
5 %TEDA/AC	37.7	54.0	8.62	0.9985	50 %

transport, which negatively impacts adsorption phenomena.

Besides, the presence of KI, even at low amounts, is expected to induce a change in adsorption kinetics. For instance, the presence of diffusional limitations associated with the existence of preferential pathways inside the adsorbent could lead to the decrease of the corresponding filtering properties, namely the adsorption capacities at breakthrough, *i.e.* the working capacity of a nuclear adsorbent [16]. In order to check this, the parameters $Q_{5\%}$ and K_{th} were plotted according to the length of the Mass Transfer Zone (MTZ) in Fig. 5. A decreasing and almost linear evolution of K_{th} towards MTZ can be noticed. Therefore, the K_{th} constant may be used to characterize the transport process of methyl iodide molecules before being adsorbed. In addition, a decreasing trend can also be outlined for the $Q_{5\%}$ values as function of MTZ at KI contents higher than 0.5 %. Thus, the presence of increasing amounts of KI (content > 0.5 wt%) seems to hinder the accessibility of some CH_3I molecules towards adsorption sites located in the micropores, leading therefore to a decrease of the working capacity of the adsorbent (Fig. 3).

Under the studied conditions ($T = 30$ °C, $\text{RH} = 0$ %), the physisorption mechanism is expected to be dominant in agreement with literature studies [11,24]. In the case of 1 %KI/AC, the weakly-adsorbed CH_3I species were evacuated at the same temperature under inert atmosphere. As all the previously-adsorbed species were removed by this simple step, it could be deduced that only physisorption phenomena, *i.e.* a fully reversible process, occur with the non-impregnated and KI-impregnated AC (see S7, in ESI). In other words, this outlines the absence of any strong interactions between KI molecules and $\text{CH}_3^{127}\text{I}$.

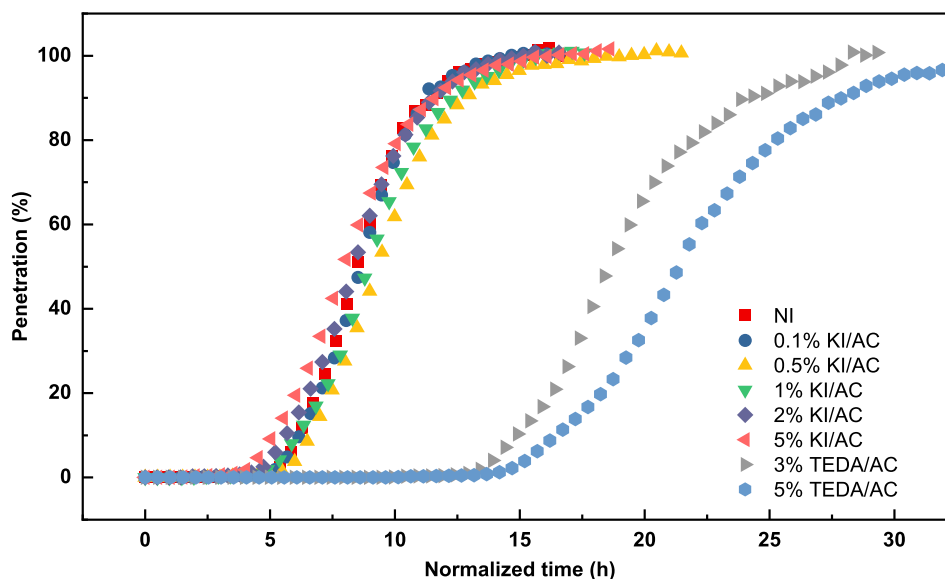


Fig. 2. BTC measured during the trapping of stable CH_3I by the different AC ($C_{\text{inlet}} = 10$ ppmv, $T = 30$ °C, bed height = 50 mm, linear velocity = $25 \text{ cm}\cdot\text{s}^{-1}$, residence time = 0.2 s). For comparative purposes, the timescale was normalized for the different reported adsorbents using an adsorbent mass of 10 g.

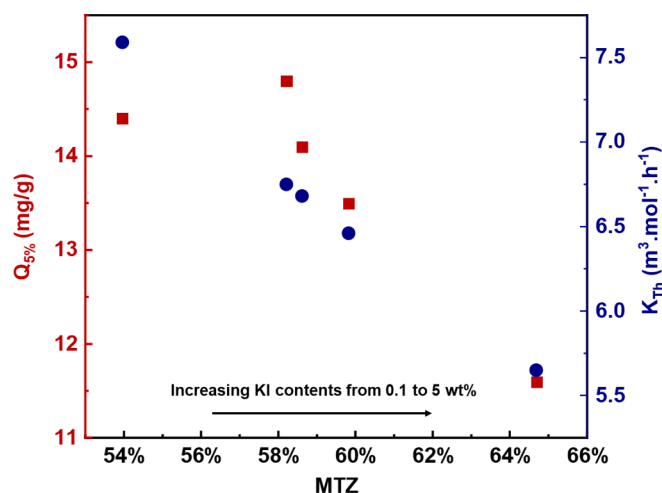


Fig. 3. Evolution of the corrected $q_{5\%}$ and K_{Th} towards the MTZ for the KI impregnated AC.

This trend is in line with our previous works under batch reactor configuration [23]. To sum-up, the behaviour of KI-impregnated AC towards the retention of stable CH_3I solely relies on non-specific interactions, themselves driven by the accessibility of the micropores for the adsorbate [23].

For TEDA-impregnated AC, a significant improvement can be observed in terms of adsorption behavior, with a total retention of about 12 h against 5 h for the non-impregnated (NI) and KI-impregnated AC (Fig. 2). This enhancement in filtering properties of 3 %TEDA/AC can be further assessed from the increase in $Q_{5\%}$ from 14.0 to 33.7 $mg \cdot g^{-1}$ and Q_{Th} from 21.3 to 47.2 $mg \cdot g^{-1}$ (as compared with non-impregnated AC). At higher TEDA content (5 wt%), an additional increase is still observed (37.7 and 54 $mg \cdot g^{-1}$ for $Q_{5\%}$ and Q_{Th} respectively, Table 1). Moreover, the incorporation of TEDA improves the trapping stability. Indeed, the fraction of physisorbed CH_3I for 5 %TEDA/AC is only about 53 % (against 100 % for KI/AC, see S7 in the ESI). The remaining fraction (about 47 %) has probably for origin the alkylation reaction between CH_3I and TEDA, to give a quaternary ammonium iodide salt [21,25]. The occurrence of strong interactions between CH_3I and TEDA was also confirmed by our previous batch reactor studies, indicating a significant enhancement of the Langmuir coefficient b in comparison with non-impregnated or KI-impregnated AC [23]. The efficiency of TEDA use for methyl iodide trapping can also be estimated from the values presented in Table 1. Once the adsorption contribution from the non-impregnated material was subtracted from adsorption capacities of TEDA/AC, a molar ratio of CH_3I /TEDA of about 0.7 and 0.5 can be deduced for 3 and 5 % TEDA/AC, respectively. Ratios below unity are expected to correspond to a non-optimal use of TEDA by the active carbon material in the current conditions [24,26].

3.3. Performances of AC adsorbents towards the trapping of γ -labelled CH_3I

3.3.1. Evolution of breakthrough curves in presence of γ -labelled CH_3I

The BTC measured for the different KI/AC adsorbents are compared for both stable and γ -labelled CH_3I on Fig. 4. In the case of radioactive methyl iodide, the BTC was fitted using the log-Thomas model (see experimental) in order to compensate for the lack of experimental points between the total retention and saturation phases. The calculated $t_{5\%}$ and $t_{95\%}$ according to this model are also reported in Table 2. Although the temperature in the experiments with γ -labelled CH_3I is slightly lower (20 °C) than with stable CH_3I (30 °C, section 3.2.), it has been verified that the changes in adsorption behaviour and adsorption parameters due to temperature effects are negligible in our operating conditions. For

comparison purpose, we have taken into account this difference of temperature when calculating the adsorption capacities towards γ -labelled CH_3I (see details in S8, ESI).

Firstly, the non-impregnated AC displays a quasi-similar behavior for the retention of radioactive and stable CH_3I , as shown by the superimposition of the breakthrough curves for $CH_3^{127}I$ (Fig. 4 a) in black)) and γ -labelled CH_3I (Fig. 4 a) in red)). For KI contents ranging between 0.1 and 0.5 wt%, the duration of the total retention phase (*i.e.* before breakthrough) seems also to be almost equal between radioactive and stable CH_3I (Fig. 4 b) and c)). However, an enhancement of the trapping properties can be observed during the breakthrough phase, resulting in calculated $t_{95\%}$ values of 20.8 and 22.4 h for 0.1 % and 0.5 % KI/AC respectively, against 14.1 h for the non-impregnated AC. An even more beneficial effect due to KI can be evidenced for contents higher than 1 wt %, considering both the duration of the total retention phase and the time needed to reach the saturation of the sorbent. Among the tested KI/AC samples, the best performances were obtained for the highest investigated KI content (5 wt%), with $t_{5\%}$ and $t_{95\%}$ of 14.3 and 52.7 h, respectively (Table 2).

This behavior is due to the isotopic exchange between ^{127}I (from KI) and ^{131}I (from γ -labelled CH_3I) [7]. Indeed, retention tests performed for 5 %TEDA/AC (see S9 in ESI) indicate similar trapping performances for stable and γ -labelled CH_3I , in agreement with the study of Wood et al. [27]. If present, the iodide salt formed following the chemical reaction between TEDA and CH_3I does not seem efficient for further exchange with radioactive methyl iodide (after dissociation), in agreement with a previous work [28]. Thus, only KI seems to play a beneficial role to enhance the γ -labelled CH_3I uptake in comparison with that of stable CH_3I . The occurrence of the exchange reaction seems to be more significant during the breakthrough phase of the tested AC. Indeed, the improvement for $t_{5\%}$ and $t_{95\%}$ is about 61 and 73 %, respectively, when comparing with the non-impregnated AC (Table 2). In comparison, the trapping of CH_3I by TEDA, presumably involving an alkylation mechanism [22,27], rather seems to occur during the retention phase (see S10). Indeed, an increase of 63 % and 53 % in $t_{5\%}$ and $t_{95\%}$ was calculated for 5 %TEDA/AC in comparison with the starting AC (Table 2).

Overall, it seems that the presence of KI and TEDA impregnants lead to different retention behavior. The presence of TEDA results in an increase in the duration of the retention phase accompanied by an enhancement in trapping stability. By contrast, the KI effect rather contributes to an increase of the length of both the retention and breakthrough phases. According to Wood et al. [27], the isotopic exchange reaction is characterized by first order kinetics.

3.3.2. Determination of the contribution of isotopic exchange at saturation of the adsorbents

In this section, we will present a first attempt to quantify the relative contribution due to isotopic exchange, which is based on the neglect of the isotopic dilution factor G_{IDF} . In other words, we assume that $CH_3^{131}I$ and $CH_3^{127}I$ retention behavior would be the same, if a $CH_3^{131}I$ concentration of 10 ppmv could have been used instead of that of $CH_3^{127}I$ in the experiments presented in section 3.2. and using GC detection.

From the results displayed in Table 1 and Table 2, a significant increase of the adsorption capacity at saturation towards $CH_3^{131}I$ can be highlighted for the KI-impregnated carbons. Taking the 5 % KI/AC as example, the Q_{Th} parameter increases from 22.8 to 70.4 $mg \cdot g^{-1}$. Considering the series of KI/AC adsorbents, this increase in adsorption capacity seems to be dependent mainly on the KI content (namely for KI content higher than 0.5 %). By contrast, no enhancement is obviously observed for the non-impregnated AC (Table 1 and Table 2), because KI is needed for isotopic exchange to take place. Hence, only physisorption is involved for the non-impregnated AC and physisorbed amounts are the same between the two configurations (stable and radioactive).

The relative contributions of physisorption and isotopic exchange are summarized in Fig. 5 for the series of KI/AC adsorbents. The gain observed in Q_{Th} parameter from about 20 % (0.1 and 0.5 % KI/AC,

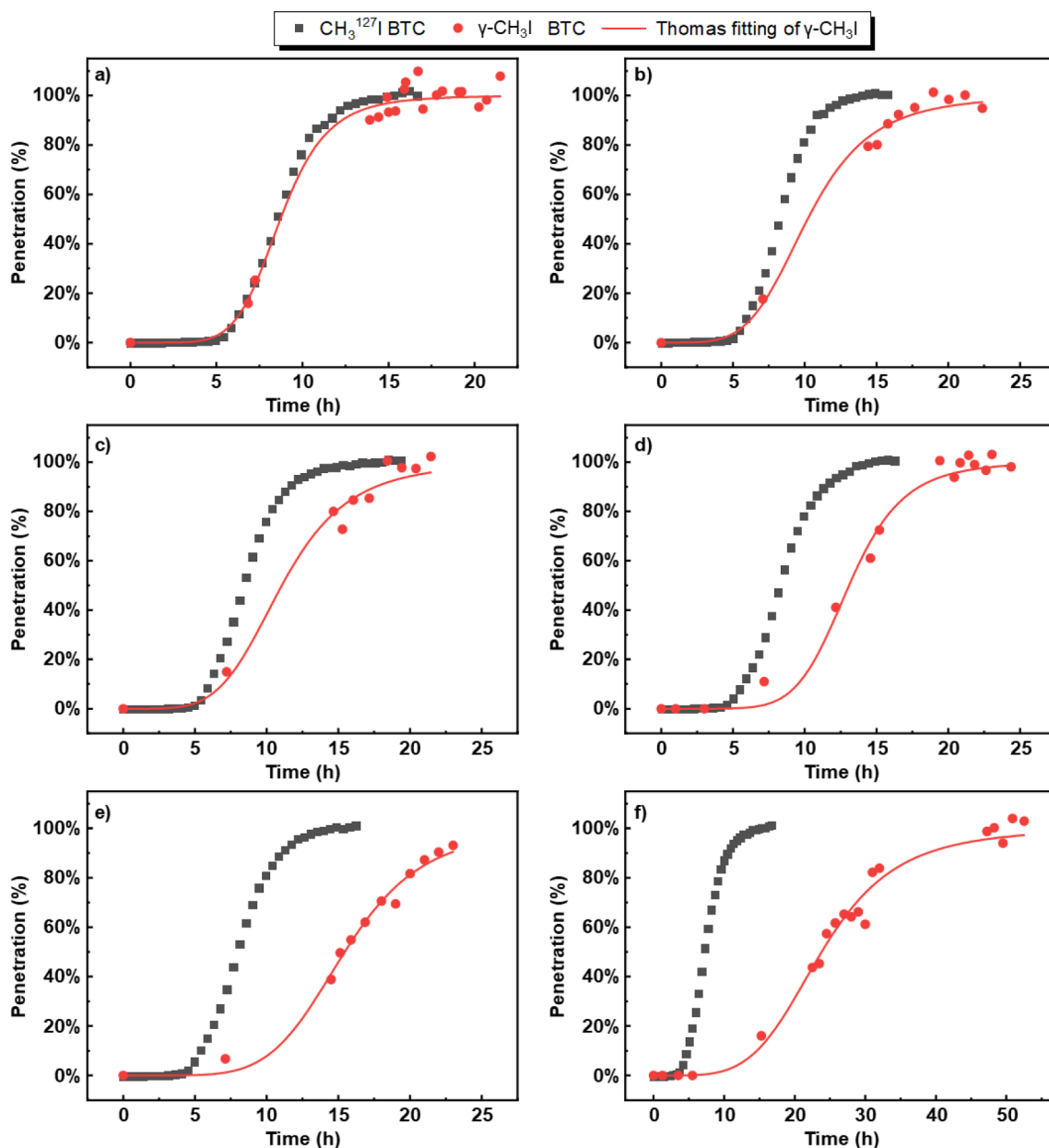


Fig. 4. Comparison between the btc measured for stable CH_3I and γ -labelled CH_3I BTC for: (a) non-impregnated AC; (b) 0.1 %KI/AC; (c) 0.5 %KI/AC; (d) 1 %KI/AC; (e) 2 %KI/AC; (f) 5 %KI/AC. Conditions for radioactive CH_3I BTC: $C_{\text{inlet}} = 10$ ppmv, $T = 20$ °C, bed height = 50 mm, $\text{CH}_3^{131}\text{I}$ flowrate around 150 Bq·min $^{-1}$, linear velocity = 25 cm·s $^{-1}$, residence time = 0.2 s.

Fig. 5) to about 72 % (5 %KI/AC, Fig. 5) between stable and radioactive CH_3I configurations is rather important. This methodology presents for the first time an approach to determine the relative contribution of isotopic exchange for nuclear adsorbents.

In the next section, the relative contribution of isotopic exchange will be further estimated using another approach.

3.3.3. Determination of the transient contribution of isotopic exchange in function of bed penetration

As stated in the previous section, the promotion of isotopic exchange in presence of impregnated KI brings interesting features to radioactive CH_3I retention, with a significant improvement of the adsorption capacity (the contribution from isotopic exchange is about 70 % for 5 %KI AC at 100 % penetration of the bed, Fig. 5). However, an AC iodine trap implemented within the ventilation networks has to be performant for radioactive iodine capture at maximal penetrations of the bed of 1–10

%, *i.e.* far away from the adsorbent saturation. Such penetrations correspond to minimal safety criteria in terms of DF between 10 and 100 (for 10 and 1 % penetration, respectively). Hence, attention should be paid to adsorbent performances at different penetrations in order to better evaluate its working capacity.

In this section, a second approach for the quantification of isotopic exchange is proposed taking this time into account the different isotopic dilution factors. Firstly, the G_{IDF} for the γ -labelled CH_3I flow is determined from experimental conditions. Similarly, the isotopic dilution factor between the adsorbed $\text{CH}_3^{127}\text{I}$ and $\text{CH}_3^{131}\text{I}$ on the surface of the KI-impregnated AC (R_{IDF}) can be determined using the following expression:

$$R_{IDF} = \frac{Q(\text{CH}_3^{131}\text{I})}{Q(\text{CH}_3^{127}\text{I})} \quad (4)$$

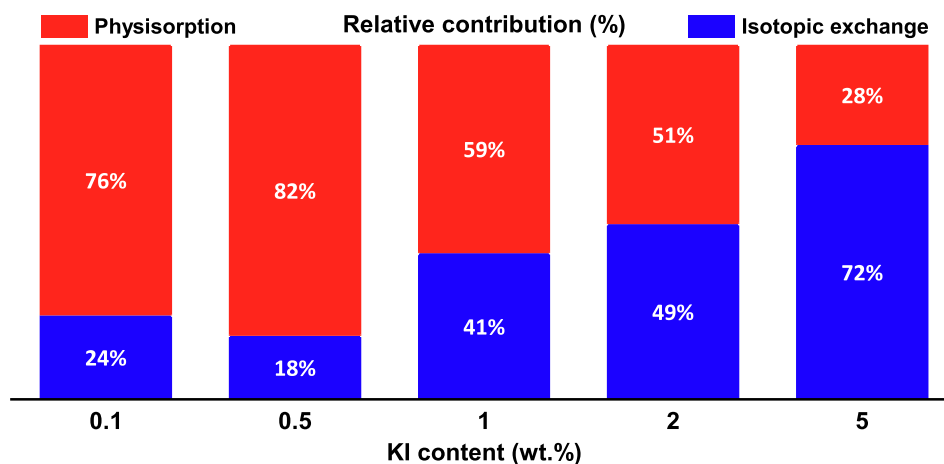


Fig. 5. Relative contribution of the isotopic exchange considering the adsorption capacity at saturation for KI impregnated AC ($(Q(\text{CH}_3^{131}\text{I}) - Q(\text{CH}_3^{127}\text{I}))/Q(\text{CH}_3^{131}\text{I})$, without G_{IDF}).

Table 2

Summary of adsorption parameters derived from BTC data measured with γ -labelled CH_3I ($\text{CH}_3^{131}\text{I}$ flowrate = $150 \text{ Bq}\cdot\text{min}^{-1}$, $T = 20^\circ\text{C}$, bed height = 50 mm, linear velocity = $25 \text{ cm}\cdot\text{s}^{-1}$, residence time = 0.2 s). The adsorption capacities are calculated for a reference adsorbent mass (10 g) and expressed at $T = 30^\circ\text{C}$ for comparison purpose with BTC measurements obtained with stable CH_3I .

AC type	$Q_{Th}(\text{mg}\cdot\text{g}^{-1})$ *	Real Q_{Th} ($\text{mg}\cdot\text{g}^{-1}$)**	Experimental breakthrough time (h) and [bed saturation level %]	Calculated $t_{5\%}$ (h)	Final t (h) and [bed saturation level]	Calculated $t_{95\%}$ (h)
NI	22.8	1.9×10^{-9}	6.9 [16 %]	5.6	21.89 [100 %]	14.1
0.1 %KI/AC	28.3	2.3×10^{-9}	7.6 [18 %]	5.8	24.05 [95 %]	20.8
0.5 %KI/AC	28.5	2.3×10^{-9}	7.8 [15 %]	6.5	23.33 [100 %]	22.4
1 %KI/AC	38.1	3.1×10^{-9}	7.8 [11 %]	11.5	26.41 [98 %]	19.3
2 %KI/AC	42.9	3.5×10^{-9}	7.7 [7 %]	9.9	24.89 [93 %]	28.1
5 %KI/AC	70.4	5.6×10^{-9}	8.6 [0.29 %]	14.3	60.4 [100 %]	52.7

*These parameters are calculated considering a $\text{CH}_3^{131}\text{I}$ concentration of 10 ppmv (without G_{IDF}).

**These parameters are calculated using the real $\text{CH}_3^{131}\text{I}$ concentration (with G_{IDF}).

Where R_{IDF} isotopic dilution factor between the adsorbed $\text{CH}_3^{127}\text{I}$ and $\text{CH}_3^{131}\text{I}$;
 $Q(\text{CH}_3^{131}\text{I})$ recalculated real $\text{CH}_3^{131}\text{I}$ adsorption capacity at a given penetration ($\text{mol}\cdot\text{g}^{-1}$) at $T = 30^\circ\text{C}$;
 $Q(\text{CH}_3^{127}\text{I})$ calculated CH_3I adsorption capacity at a given penetration ($\text{mol}\cdot\text{g}^{-1}$).

This isotopic dilution factor within the adsorbed phase R_{IDF} is then determined from the fitted BTC according to the improved Thomas model (see experimental) for radioactive and stable experiments. Transient adsorption capacities were calculated for both configurations, each corresponding to a given filter breakthrough.

The isotopic exchange process for the KI-impregnated AC induced an enrichment in adsorbed $\text{CH}_3^{131}\text{I}$ compared with adsorbed $\text{CH}_3^{127}\text{I}$ inside the AC (as witnessed from the computed R_{IDF} values). Therefore, the value of the R_{IDF} can be compared with the initial gaseous phase composition G_{IDF} to determine the relative contribution due to isotopic exchange using the following expression:

$$\text{Relativecontribution}(\%) = \frac{R_{IDF} - G_{IDF}}{R_{IDF}} \quad (5)$$

Since the transient adsorption capacity (at a given breakthrough) was proportional to $\text{CH}_3^{131}\text{I}$ inlet concentration (see S8, ESI), the following expression could be obtained:

$$Q(\text{CH}_3^{131}\text{I}) = Q(\text{CH}_3^{127}\text{I}) \times G_{IDF} \quad (6)$$

Here, the $Q(\text{CH}_3^{127}\text{I})$ is the adsorption capacity calculated for inlet $\text{CH}_3^{131}\text{I}$ concentration of 10 ppmv and recalculated at $T = 30^\circ\text{C}$. Using

Eq. (4) and Eq. (5), the Eq. (6) can be reformulated as:

$$\text{Relativecontribution}(\%) = \frac{Q(\text{CH}_3^{131}\text{I}) - Q(\text{CH}_3^{127}\text{I})}{Q(\text{CH}_3^{131}\text{I})} \quad (7)$$

Hence, Eq. (7) can be used to calculate the transient adsorption capacity at a given penetration for γ -labelled CH_3I . In other words, the contribution of isotopic exchange can be determined at any filter breakthrough level.

Based on this methodology, the contribution of isotopic exchange at different levels of $\text{CH}_3^{131}\text{I}$ penetration is presented on Fig. 6 (a) and (b).

According to Fig. 6 (a), the relative contribution of isotopic exchange to the adsorption process exhibit different regimes for all KI/AC adsorbents. For 5 %KI/AC, this contribution increases from 60 to 72 % at penetrations of 25 and 100 %, respectively. Above 25 % penetration, the increase is generally less rapid and is almost linear, especially at KI concentrations higher than 1 wt%. A closer look to Fig. 6 (b) (presented in logarithmic scale), provides information for the low penetration values in agreement with the nuclear context of interest. In fact, the contribution of isotopic exchange can be evidenced experimentally only above a certain penetration (from less than 0.1 % up to 10 % depending on the adsorbent). This threshold depends both on KI content but also to some limitations pertaining to the present methodology. Indeed, increasing the KI content will enhance both the durations of the total retention and breakthrough phases, as previously stated. For those adsorbents with KI content of 1 wt% and above, the experimental points that were measured between the retention and the saturation phases are more important than for the other adsorbents (Fig. 4). In other words, the extrapolation of isotopic exchange relative contribution to

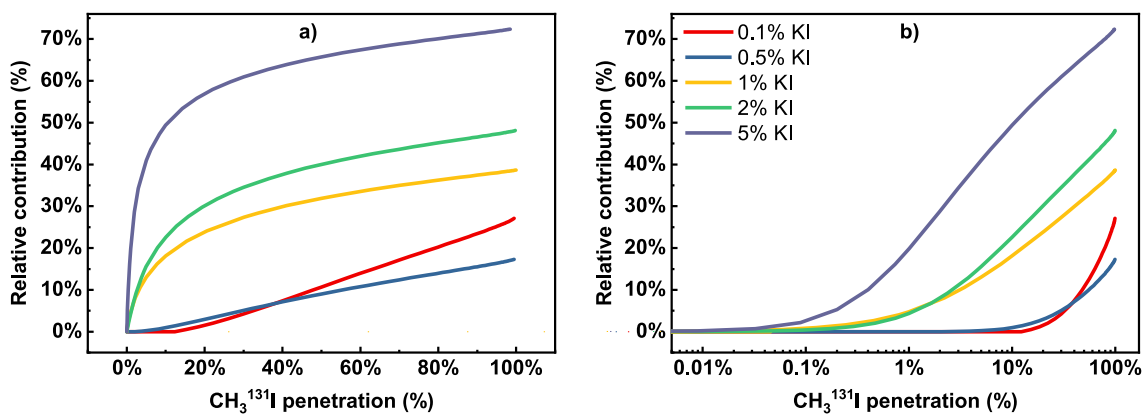


Fig. 6. Evolution of the relative contribution due to the isotopic exchange in function of $\text{CH}_3^{131}\text{I}$ penetration: (a) penetration in linear scale; (b) penetration in logarithmic scale.

penetrations less than or equal to 10 % cannot be feasible for 0.1 wt% and 0.5 wt% KI AC considering the lack of the experimental data for the improved Thomas model fitting (Fig. 4).

The relative contribution due to isotopic exchange at low penetrations (1 %, 5 % and 10 %) are therefore presented only for the most efficient adsorbents (2 %KI and 5%KI/AC, see S11). From the results summarized in S11, the calculated relative contribution due to the isotopic exchange at 1 % of $\text{CH}_3^{131}\text{I}$ penetration is not neglectable (4 and 20 % for 2 %/KI and 5 %/KI AC, respectively). These first calculations outline the importance of isotopic exchange phenomena for KI/AC adsorbents even at low penetrations.

4. Conclusions

The main purpose of this study was to evaluate qualitatively and quantitatively the contribution of isotopic exchange to the overall retention of radioactive CH_3I by different kinds of *nuclear-grade* activated carbon (AC) sorbents. The methodology involves the accurate measurements of breakthrough curves (BTC) with both stable and γ -labelled CH_3I separately through two different experimental setups.

Regarding stable CH_3^{27}I trapping, similar performances were measured for the non-impregnated and KI-impregnated AC with calculated adsorption capacity of about 20 mg/g ($C_0 = 10$ ppmv). This is logical considering their similar textural properties and an adsorption process driven by only physical or non-specific interactions between CH_3I and the adsorbent surface (reversible fraction of about 100 %).

When considering the adsorption of a γ -labelled CH_3I flow of equal concentration (10 ppmv), but containing both $\text{CH}_3^{131}\text{I}$ and $\text{CH}_3^{127}\text{I}$, the presence of KI, especially at contents above 1 wt%, leads to the increase of retention performances, as compared with the non-impregnated AC. The KI effect is due to the isotopic exchange reaction. Indeed, additional tests have indicated the absence of a such phenomenon for the non-impregnated material and 5 %TEDA AC.

For the first time, we were able to isolate and quantify the contribution of isotopic exchange for different kinds of KI/AC nuclear adsorbents. Two complementary methodologies were designed to quantify this contribution. First, the importance of isotopic exchange was quantitated at saturation of the adsorbents, corresponding to a bed penetration of 100 %. Hence and in comparison with the non-impregnated AC, additional retentions of 18 (0.5 %KI/AC) to 72 % (5 %KI/AC) were calculated depending on the KI content. On the other hand, a more valuable expression of this contribution in function of γ - CH_3I penetration was established. Hence, transient contributions corresponding to maximal bed penetrations of 1–10 %, could also be determined. These values are of more practical use considering nuclear applications where saturation of adsorbed bed by CH_3I is never reached. More precisely, the extrapolation to a penetration of 1 % through the use of an improved

Thomas model for both stable and radioactive CH_3I sorption profiles, has allowed to estimate relative contributions of about 4 % and 20 % for 2 %KI/AC and 5 %KI/AC, respectively.

Declaration of Competing Interest

The authors declare that they have no known competing financial interests or personal relationships that could have appeared to influence the work reported in this paper.

Data availability

Data will be made available on request.

Acknowledgements

The research leading to these results is partly funded by the Institut de Radioprotection et de Sûreté Nucléaire (IRSN). This work was performed within the “Iodine” research program of the IRSN.

Appendix A. Supplementary data

Supplementary data to this article can be found online at <https://doi.org/10.1016/j.seppur.2023.125427>.

References

- [1] B. Clement, L. Cantrel, G. Ducros, F. Funke, L. Herranz, A. Rydl, G. Weber, C. Wren, State of the art report on iodine chemistry, NEA/CSNI/R(2007)1, 2007.
- [2] D. Haefner, T. Tranter, Methods of gas phase capture of iodine from fuel reprocessing off-gas: a literature survey, Idaho National Laboratory (2007), <https://doi.org/10.2172/911962>.
- [3] R.T. Jubin, A literature survey of methods to remove iodine from off-gas streams using solid sorbents, Oak Ridge National Laboratory. ORNL/TM-6607, Oak Ridge, TN, 1979.
- [4] C.Y. Yin, M.K. Aroua, W.M.A.W. Daud, Review of modifications of activated carbon for enhancing contaminant uptakes from aqueous solutions, Sep. Purif. Technol. 5 (2007) 403–415, <https://doi.org/10.1016/j.seppur.2006.06.009>.
- [5] C.M. Ecob, A.J. Clements, P. Flaherty, J.G. Griffiths, D. Nacapricha, C.G. Taylor, Effect of humidity on the trapping of radioiodine by impregnated carbons, Sci. Total Environ. 130–131 (1993) 419–427, [https://doi.org/10.1016/0048-9697\(93\)90096-0](https://doi.org/10.1016/0048-9697(93)90096-0).
- [6] B. Collinson, L. R. Taylor, P. Meddings, Trapping performance of 1.5% KI 207B charcoal for methyl iodine in CO_2 at high temperature and pressure, In : Proceedings of the 20th DOE/NRC nuclear air cleaning conference. Sessions 1-5, pp. 537–559, 1989.
- [7] J. Huve, A. Ryzhikov, H. Nouali, V. Lalia, G. Augé, T.J. Daou, Porous sorbents for the capture of radioactive iodine compounds: a review, RSC Adv. 8 (2018) 29248–29273, <https://doi.org/10.1039/C8RA04775H>.
- [8] V.R. Deitz, Interaction of radioactive iodine gaseous species with nuclear-grade activated carbons, Carbon 25 (1987) 31–38, [https://doi.org/10.1016/0008-6223\(87\)90037-6](https://doi.org/10.1016/0008-6223(87)90037-6).

- [9] J. Zhou, S. Hao, L. Gao, Y. Zhang, Study on adsorption performance of coal based activated carbon to radioactive iodine and stable iodine, *Ann. Nucl. Energy* 72 (2014) 237–241, <https://doi.org/10.1016/j.anucene.2014.05.028>.
- [10] K. Ho, S. Moon, H.C. Lee, Y.K. Hwang, C.H. Lee, Adsorptive removal of gaseous methyl iodide by triethylenediamine (TEDA)-metal impregnated activated carbons under humid conditions, *J. Hazard. Mater.* 368 (2019) 550–559, <https://doi.org/10.1016/j.jhazmat.2019.01.078>.
- [11] K. Ho, H. Chun, H.C. Lee, Y. Lee, S. Lee, H. Jung, B. Han, C.-H. Lee, Design of highly efficient adsorbents for removal of gaseous methyl iodide using tertiary amine-impregnated activated carbon: Integrated experimental and first-principles approach, *Chem. Eng. J.* 373 (2019) 1003–1011, <https://doi.org/10.1016/j.cej.2019.05.115>.
- [12] F. Kepak, Removal of gaseous fission products by adsorption, *J. Radioanal. Nucl. Chem.* 142 (1990) 215–230, <https://doi.org/10.1007/BF02039464>.
- [13] H. Lin, M. Chebbi, C. Monsanglant-Louvet, B. Marcillaud, A. Roynette, D. Doizi, P. Parent, C. Laffon, O. Grauby, D. Ferry, KI and TEDA influences towards the retention of radiotoxic CH₃I by activated carbons, *J. Haz. Mater.* 431 (2022), 128548, <https://doi.org/10.1016/j.jhazmat.2022.128548>.
- [14] M. Chebbi, B. Azambre, C. Monsanglant-Louvet, B. Marcillaud, A. Roynette, L. Cantrel, Effects of water vapour and temperature on the retention of radiotoxic CH₃I by silver faujasite zeolites, *J. Haz. Mater.* 409 (2021), 124947, <https://doi.org/10.1016/j.jhazmat.2020.124947>.
- [15] V. J. Inglezakis, S. G. Pouloupoulos, *Adsorption, Ion Exchange and Catalysis: Design of Operations and Environmental Applications*. Elsevier, 2006.
- [16] M. Chebbi, B. Azambre, L. Cantrel, M. Huvé, T. Albiol, Influence of structural, textural and chemical parameters of silver zeolites on the retention of methyl iodide, *Microporous Mesoporous Mater.* 244 (2017) 137–150, <https://doi.org/10.1016/j.micromeso.2017.02.056>.
- [17] H. Lin, *Evaluation de la contribution du mécanisme d'échange isotopique à l'épuration de l'iode radioactif*, Sorbonne university, 2022. PhD thesis.
- [18] H.C. Thomas, Heterogeneous ion exchange in a flowing system, *J. Am. Chem. Soc.* 66 (1944) 1664–1666, <https://doi.org/10.1021/ja01238a017>.
- [19] R. Apiratikul, K.H. Chu, Improved fixed bed models for correlating asymmetric adsorption breakthrough curves, *J. Water Process Eng.* 40 (2021), 101810, <https://doi.org/10.1016/j.jwpe.2020.101810>.
- [20] J.M. López, M.V. Navarro, T. Garcia, R. Murillo, A.M. Mastral, F.J. Varela-Gandia, D. Lozano-Catsetillo, A. Bueno-Lopez, D. Cazorla-Amoros, Screening of different zeolites and silicoaluminophosphates for the retention of propene under cold start conditions, *Microporous Mesoporous Mater.* 130 (2010) 239–247, <https://doi.org/10.1016/j.micromeso.2009.11.016>.
- [21] S.W. Park, W.K. Lee, H. Moon, Adsorption and desorption of gaseous methyl iodide in a triethylenediamine-impregnated activated carbon bed, *Sep. Technol.* 3 (1993) 133–142, [https://doi.org/10.1016/0956-9618\(93\)80013-H](https://doi.org/10.1016/0956-9618(93)80013-H).
- [22] H.-K. Lee, G.-I. Park, Adsorption characteristics of elemental iodine and methyl iodide on base and TEDA impregnated carbon, *Nucl. Eng. Technol.* 28 (1996) 44–55.
- [23] M. Chebbi, C. Monsanglant-Louvet, P. Parent, C. Gerente, L. Le Coq, B.M. Mokili, Sorption properties of activated carbons for the capture of methyl iodide in the context of nuclear industry, *Carbon Trends* 7 (2022), 100164, <https://doi.org/10.1016/j.cartre.2022.100164>.
- [24] G.-I. Park, I.-T. Kim, J.-K. Lee, S.-K. Ryu, J.-H. Kim, Effect of temperature on the adsorption and desorption characteristics of methyl iodide over TEDA-impregnated activated carbon, *Carbon Lett.* 2 (2001) 9–14.
- [25] E. Aneheim, D. Bernin, M.R. StJ, Foreman, Affinity of charcoals for different forms of radioactive organic iodine, *Nucl. Eng. Des.* 328 (2018) 228–240, <https://doi.org/10.1016/j.nucengdes.2018.01.007>.
- [26] K. Ho, D. Park, M.-K. Park, C.-H. Lee, Adsorption mechanism of methyl iodide by triethylenediamine and quinuclidine-impregnated activated carbons at extremely low pressures, *Chem. Eng. J.* 396 (2020), 125215, <https://doi.org/10.1016/j.cej.2020.125215>.
- [27] G. O. Wood, F. O. Valdez, Nonradiometric and radiometric testing of radioiodine sorbents using methyl iodide, In : *Proceedings of the 16th DOE Nuclear Air Cleaning Conference*, pp. 448–464, 1980.
- [28] Y.S. Kim, A study on adsorption characteristics and deterioration patterns of an impregnated active carbon under a simulated service condition of the filtering system at a nuclear power plant. In : *Proceeding of the 20th DOE/NRC Nuclear Air Cleaning Conference*, Boston, MA, USA, 22 Aug, 1988.